Chapter 2
State of the Art

A comprehensive literature review on biomechatronics input interfaces was carried out to identify the key issues in this field. The main design requirements and development complications were identified and the various approaches used in past interfaces were reviewed. The review begins with a survey of existing biological interfaces designed for use in human assistance and treatment. An overview of EEG and EMG based biomechanical models is also provided. This is followed by a review of the state-of-the-art in biomechanical model-based control strategies, with primary focus on its application to rehabilitation robots. Finally, the reviewed materials are discussed to highlight issues in biomechanics that require further work, and are hence the subject of investigation for this research.

2.1 EEG-Based BCI and Its Challenges

2.1.1 Steady State Visual Evoked Potentials

The signal sources of BCIs can be categorised by whether they use evoked or spontaneous inputs. Evoked inputs are those caused by external triggers, for example VEPs are produced in the visual cortex by flashing lights, and P300 signals appear about 300 ms after the presentation of "novel" stimuli. Spontaneous inputs are those produced as part of the normal functioning of the brain. These, therefore, must include signals from every part of the brain for all its functions; whether they are detectable or able to be interpreted is another issue. An example is rhythms in the EEG around the sensorimotor cortex, which are commonly used as they are associated with actual or imagined movement. Next, we look in detail at relevant evoked and spontaneous inputs used in various BCI systems.

S. Xie and W. Meng, *Biomechatronics in Medical Rehabilitation*,
DOI 10.1007/978-3-319-52884-7_2

Slow cortical potentials

SCPs and neural oscillations (alpha, beta, mu, and gamma rhythms) are commonly referred to as brain waves. These rhythms involve the synchronised firing of large numbers of neurons, and are associated with changes in state of consciousness such as attention and sleep. In normal brain function, negative SCPs reflect preparatory depolarisation of the underlying cortical network, whereas positive SCPs are usually interpreted as a sign of cortical disfacilitation or inhibition. Figure 2.1a illustrates a SCP signal used by a BCI. It lasts from 300 ms to several seconds. With appropriate training, users can learn to control SCPs to move a cursor to a target at the bottom of a computer screen (more positive SCP) or top (more negative SCP) of a computer screen [1, 2]. They can use this control to perform basic word processing and other simple tasks such as browsing the Internet. Most importantly, people who are severely disabled and are otherwise unable to communicate, are capable of using SCP for control and communication. Detecting and classifying these signals is relatively easy because they are strong and consistent. However, generating these signals generally requires concentration from the user, the number of control DOFs is limited to the number of rhythms the user can be trained to control, and the response is often slow.

P300 potentials

A P300 evoked potential is a positive potential generated about 300 ms after a novel trigger signal is flashed on a screen. An example of a P300 VEP is shown in Fig. 2.1b [3, 4]. Typically, a matrix of possible selections (letters or symbols) is shown on a screen. Scalp EEG is then recorded over the centro parietal cortex while these selections flash in rapid succession. Only the flashing of the letter or symbol, which the user wants to select, produces a P300 potential because this signal is unusual when compared to the other symbols. By detecting this P300 potential, the BCI system can determine the user's choice. This BCI method can support a simple word processing program, enabling users to write words at a rate of a few letters per minute. Improvements in signal analysis may substantially increase the capabilities of a P300 word processor. However, the effects of long-term usage of a P300-based BCI are unknown. Its reliability may improve with practice, or the brain may become used to the stimulation and produce a smaller signal.

Sensorimotor rhythms

Sensorimotor rhythms (SMR) are oscillations in the EEG recorded over the sensorimotor cortices. The oscillation frequencies of interest are in the 8–12 Hz range (mu waves) and 18–26 Hz range (beta waves). The sensorimotor cortices are an area of the outermost layer of the brain, the cerebral cortex, which is involved in the processing of sensory information, planning, control, and execution of voluntary movements.

Changes in mu or beta rhythm amplitudes are associated with movement, sensation, and motor imagery. Motor imagery is imagined movement such as thinking about performing a golf swing. Several research groups have shown that people can

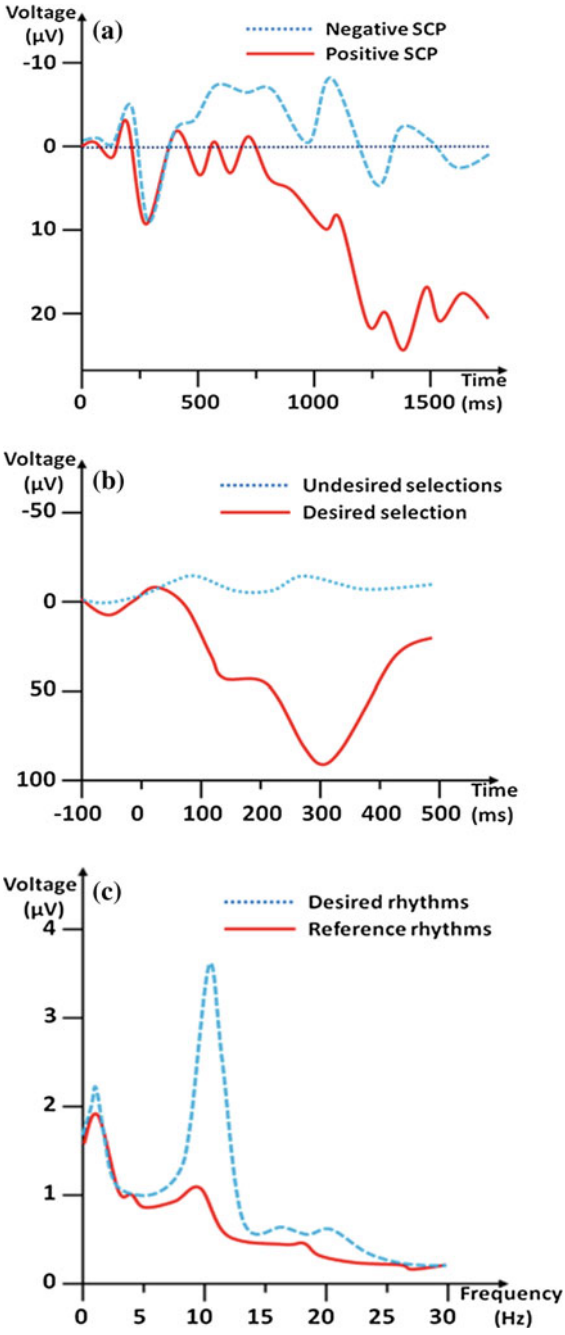

Fig. 2.1 Three kinds of signal sources in EEG-based BCIs (Modified from [1]): **a** SCPs [1, 2], **b** P300 evoked potential [3, 4], and **c** the frequency pattern of SMR [5, 6]

learn to control mu or beta rhythm amplitudes in the absence of movement or sensation [7–9], as can be seen in Fig. 2.1c, where a BCI based on SMR is illustrated. Like the P300 and SCP-based BCIs, SMR BCIs can support basic word processing or other simple functions. Trained users can also achieve multi-DOF control of a robotic arm or wheelchair [5].

Steady state visual evoked potentials

An EEG evoked potential (EP) is a distinctive EEG signal produced a repeatable time after a specific sensory stimulus or event. Visual EPs are signals that are evoked by a visual stimulus. Examples of visual stimuli are a flash of light, change in colour, or the appearance of an image. The most prominent signals are the N70 and P100 [10], so named because they are generated in the primary visual cortex approximately 70 and 100 ms after the visual stimulus. Steady state VEPs are the stable oscillations generated when the visual stimulus is applied rapidly and repetitively by a strobe light, flickering LEDs (light-emitting diodes), or a reversing checkerboard pattern on a monitor. Frequency analysis of the resulting SSVEPs shows peaks at the stimulation frequency as well as higher harmonics [11].

To create a BCI, the user is usually presented with several stimuli flickering rapidly at different frequencies. By selecting an option, users focus their gaze on the stimulus that represents the desired option. The resulting EEG signal is then time averaged to reduce noise and non-CNS artefacts, and the strongest signal matching the targeted stimulus frequency is used as the output. This is the standard and easiest method to implement a SSVEP BCI, but there are alternatives such as flashing each stimulus one at a time, or flashing the stimulus in a pseudo-random pattern [12]. This second alternative does not strictly generate SSVEPs as it does not produce steady state outputs [11].

SSVEP systems can be used to control a variety of devices, with 64 or more simultaneous stimuli to control a complex menu [13], four stimuli to control the movement of a computer avatar in two DOF [14–16], assist a disabled user to participate in an active rehabilitation exercise [17], or play a video game [18]. Although this could be interpreted as simply an eye tracking system, it has become clear that SSVEPs are not entirely dependent on what the eye is pointing at. Indeed, even without users directly pointing their eyes at the stimulus, a SSVEP-based BCI can function based on what the user is consciously focusing on [19, 20]. BCIs based on SSVEPs have the advantage that, unlike eye tracking methods, they are not affected by rapid eye movements that occur even when the eye is focused on an object. Further, with SSVEP BCI methods, multiple stimuli can be closely spaced in the visual field [11].

2.1.2 EEG Signal Processing: Improving the SNR

EEG-based BCIs use the electrical signals generated by the user's brain activity to determine their intent. The key determinant of a signal feature's value is its correlation

with the user's intent. Therefore, it should be detectable, controllable, and repeatable. The ability of a BCI to detect these features, similar to that of other communication systems, depends on the SNR. In order to boost the SNR to achieve higher BCI detection performance, the user can consciously try to improve the quality of the feature generated, and the system can try to remove as much noise as possible.

Electrodes

To increase the SNR of EEG-based BCIs, selecting the right electrodes is very important, especially with older EEG systems, which require low impedances of less than 10 kΩ. To achieve impedances this low, the scalp must usually be abraded and a conductive gel or paste applied between the scalp and electrode. Modern EEG systems can tolerate impedances of 30–50 kΩ without degrading performance, but with the disadvantage of increased amplitude power-line artefacts. In these modern systems sponge-saline electrodes can be used instead of conductive gel. The former have the advantage of faster and cleaner application but have a limited recording time because they dry out. Due to these problems, work is being done to create dry electrodes that can be applied easily, are robust in everyday use, and work all day. Such electrodes would be a significant advance for BCI systems. However, the technology is not yet fully developed [11].

Removing non-CNS artefacts

EEG artefacts are noise from any source not originating in the brain and spinal cord (together the CNS). Since artefacts are generally several orders of magnitude larger than actual EEG signals, one of the main problems in EEG analysis is the detection and removal of them, so that its classifying algorithms can function correctly. There are five main sources of artefacts: EEG equipment; changes in skin resistance due to sweating and variation in electrode pressure; displacement of the electrodes relative to the brain; external electromagnetic fields due to power-line noise; and muscle activity [21, 22].

Previous studies have shown that the most severe of the artefacts are due to muscle movements (EMG) and eye movements and blinks (electrooculography, EOG) [23, 24]. At the frontal, temporal, and occipital locations on the scalp, the magnitude of EMG or EOG signals can be greater than EEG, even in characteristic EEG frequency bands [21, 25]. Gupta and colleagues used a fixed band-pass FIR (finite impulse response) filter and a specific artefact threshold to find and remove artefacts in EEG signals [26], as shown in Fig. 2.2. This method has the advantage of working when there is a baseline drift and can be implemented in a real-time system. However, it fails if the subject's eye blink rate is unnaturally high, and the training session for each subject is quite long.

Signal representation

After removing as many artefacts as possible, the EEG signal can then be processed to improve the resolution of the resulting data, or to isolate particular signals of interest. To choose the best method to maximise the SNR, a way to compare alternative methods is essential. A statistical measure useful in such comparisons is r^2,

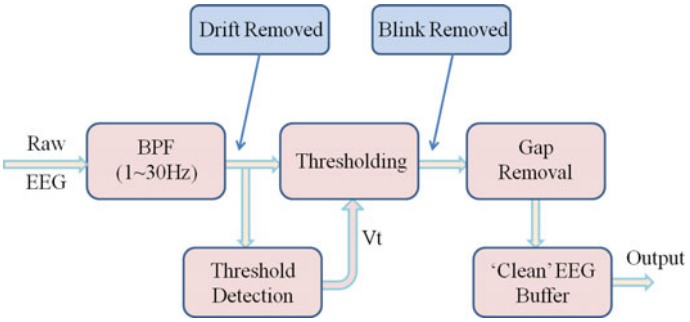

Fig. 2.2 Block diagram of an FIR filter for removing artefacts in an EEG BCI. First, the raw EEG samples are passed through a digital band-pass filter (BPF) to remove any baseline drift. Second, the artefact threshold (Vt) for a specific subject is determined in a brief training session. Third, the absolute sample value is compared with Vt. Fourth, if the value is exceeded then N samples will be removed from the vicinity of the zero crossing (defined as N/2 either side of the threshold crossing). Fifth, the following N samples are shifted to fill up the gap created by blink removal. If this last step is not done, these gaps grossly distort the spectrum

which is a measure of how well the desired outcomes are predicted by a model. However, in trying to make a true brain computer interface, it is essential to be sure that such a high r^2 is not being achieved by non-CNS artefacts, such as EMG or EOG. A final consideration is that a method with a high r^2 in offline testing may not perform as well in an online experiment.

The magnitude of the Fourier Transform (FT) of the signal has spectral information but no temporal information. Frequency-based features are widely used because of their ease of application, computational speed, and direct interpretation of the results. Specifically, about one-third of BCI designs use power-spectral features. Due to the non-stationary nature of the EEG signals, these features do not provide any time domain information. Thus, mixed Time-Frequency Representations (TFRs) that map a one dimensional (1D) signal into a two dimensional (2D) function of time and frequency are used to analyse the time-varying spectral content of the signals. It has been shown that TFR methods may yield performance improvements compared to the traditional FT-based methods [27, 28]. Most of the BCI designs that employ TFR methods use a wavelet-based feature extraction algorithm. The choice of the particular wavelet used is a crucial factor in gaining useful information from the analysis. Prior knowledge of the physiological activity in the brain can be useful in determining the appropriate wavelet function. Correlative TFR (CTFR) is another time-frequency representation method that does not only provide the spectral information, but also provides information about the time-frequency interactions between the components of the input signal. Thus, with the CTFR, EEG data samples are not independently analysed, but their relationship is also taken into account. Nevertheless, the CTFR is relatively sensitive to noise. Consequently, the values of the CTFR most relevant to signal analysis must be selected [29].

Dimensionality reduction algorithms can be used to find the most informative features and can therefore reduce the complexity of the classification problem. The experiments of [30, 31] demonstrate that when dimensionality reduction is used the classification accuracy is improved. Principal component analysis (PCA) and GAs are the most frequently used dimensionality reduction methods in BCIs. PCA retains lower order principal components and ignores higher-order ones. Such low order components often contain the most important aspects of the data. PCA only finds linear subspaces; it also works best if the individual components have Gaussian distributions, and is not optimised for class separability. GAs have demonstrated substantial improvement over a variety of random and local search methods [32]. Since GAs are domain-independent search techniques, they are ideal for applications where domain knowledge and theory is difficult or impossible to provide. An important step in developing a GA-based search is defining a suitable fitness function. An ideal fitness function correlates closely with the algorithm's goal, and is quickly computed. Definition of the fitness function is not straightforward in many cases and is usually performed iteratively if the fittest solution produced by a GA is not the desired one.

2.1.3 EEG Signal Processing: Signal Translation and Classification

In order to produce a useful output, a BCI system must convert signal features in the EEG into device control commands. These commands may be discrete (for example, icon selection) or continuous (for example, cursor movements). They should also be decoupled from each other. For instance, vertical cursor movement and horizontal cursor movement should not depend on each other. The success of a translation algorithm is determined by the appropriateness of its selection of signal features and by how effectively it translates this into device commands. As the function of most translation algorithms is to classify signal features into various categories, they are called classifiers.

Classifiers

Linear classifiers are generally more robust than nonlinear ones because linear classifiers have fewer parameters to tune, and are thus less prone to over-fitting [33]. The most commonly used techniques are linear discriminant analysis (LDA) [27] and threshold detection [34]. Strong noise and outliers can still cause linear systems to fail. One way of overcoming this problem is to use regularisation, which helps limit the influence of outliers and strong noise; the complexity of the classifier; and the raggedness of the decision surface [33].

When there are large amounts of data and complex relationships between the variables, nonlinear methods, for example neural networks (NNs) [35, 36] are more suitable. Many nonlinear methods have a large number of parameters to tune, which is difficult if the relationships between variables are poorly understood, as in the case

of EEG. This means that nonlinear methods such as NNs are used. These methods are distinguished by their ability to tune parameters within a large search space.

Kernel-based classifiers maintain all the benefits of linear classification when the overall classification is nonlinear. They work by applying a linear classification in some appropriate (kernel) feature space. Examples of such kernel-based classification methods are support vector machines (SVMs) [37] and the Kernel Fisher Discriminant (KFD) [33].

The previously mentioned systems do not take into account temporal information in the input data. Classification rates can be improved with algorithms such as finite impulse response and multi-layer perceptron neural networks (FIR-MLPNN) and tree based neural networks (TBNN) that are presented in [38]. The motivation for using such classifiers is that the patterns to be recognised are not static but time series. Thus, the temporal information of the input data can be used to improve the classification results [38].

Improving classification accuracy

BCIs are prone to errors in the recognition of the subject's intent, and these errors can be very frequent. Even with substantial training, subjects are unlikely to achieve a 100% success rate. Therefore, reducing errors, or reducing the effect of errors is one of the most important steps to making BCIs more practical. A number of groups have been exploring different ways to improve the performance of BCIs [39]. Wolpaw and his colleges found one possible technique to reduce errors. This involves a verification procedure whereby each output requires two opposite trials, and success is required on both to validate the outcome [40]. Even if this method greatly reduces the errors, it requires much more mental effort from the subject and halves the communication rate.

A group (committee) of classifiers usually yields better classification accuracy than any individual classifier could provide. Only a few BCI designs have employed such an approach in classifying features and achieved performance improvements [41, 42]. The classification accuracy of the committee depends on how much unique information each committee member contributes to classification. That is, a committee of classifiers using very similar classification techniques is unhelpful because they will produce identical answers. A committee can also be used to combine information from several channels, each receiving EEG signals from different spatial regions on the brain [43].

Classification techniques should reduce the over-fitting of a BCI system to the specific datasets used in training, otherwise, it is unlikely to function well in the real world. This is most important when different versions of a certain classification design are being compared, and the number of epochs available for evaluating the system is small. K-fold cross-validation and statistical significance tests are useful for these cases [35, 37]. K-fold cross-validation can be used to estimate the generalisation error of a given model, or it can be used for model selection by choosing the model that has the smallest estimated generalisation error. Usually, a value of 5–10 for K is recommended for estimating the generalisation error. Unfortunately, these techniques are not suitable for online evaluations.

A learning process is usually incorporated into BCI to adapt the system to different users, as well as to maintain or improve performance over time. The human brain is highly adaptable, or plastic. At the same time as the BCI system is adapting to the user, the user's brain will also be adapting to the new output from the BCI. Thus, the process of mutual adaptation of the user to the system, and the system to the user is likely to be a fundamental feature of the operation of any successful BCI system [44, 45].

Error related potentials

One useful way to improve the accuracy of a classifier over time is the error related potential (ErRP). This is a signal visible in the EEG after the user perceives an error has been made, as shown in Fig. 2.3 [46, 47]. The ErRP most likely originates in a brain area called the pre-supplementary motor area (pre-SMA) (Fig. 2.4) and anterior cingulate cortex (ACC), which are areas that are involved in regulating emotional responses [48].

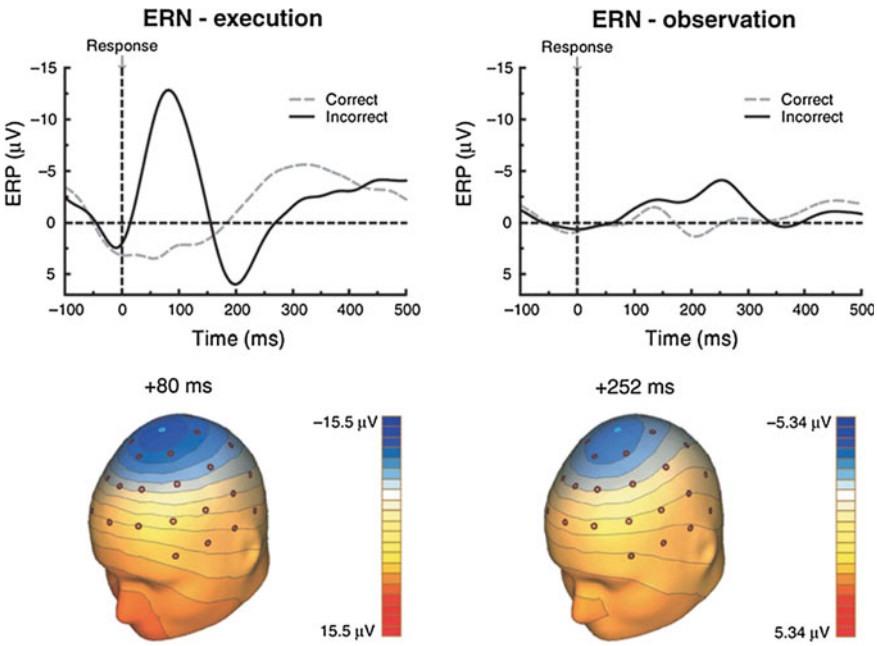

Fig. 2.3 Error-related negativities (ERNs). *Upper* Response-locked averages at electrode Cz for correct and incorrect responses in the execution condition (*left*) and the observation condition (*right*). *Dashed grey lines* indicate correct, and *solid black lines* indicate incorrect response trials. *Lower* Spline maps showing the topography of the ERN difference wave in the execution condition and the observation condition, taken at the peak where correct and incorrect ERPs differed maximally by 80 and 252 ms after the response, respectively. The Cz electrode at the vertex is marked in *light blue* for reference (Image from [49])

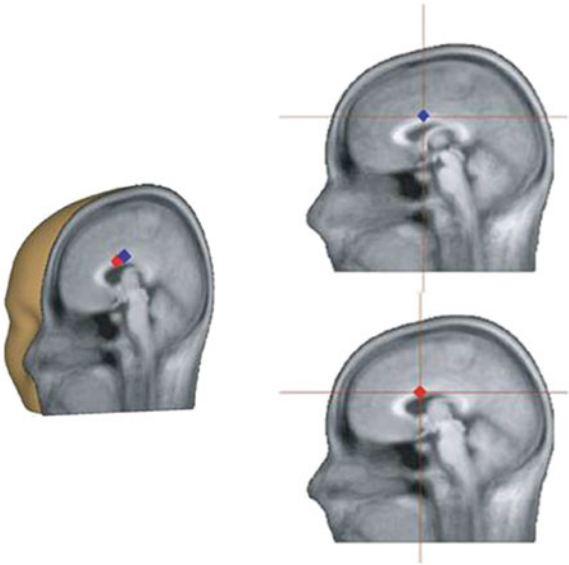

Fig. 2.4 Sagittal view of the brain showing the source for the ErRP difference wave in the execution condition (*blue*) and in the observation condition (*red*). These are displayed together within the same head model (*left*) and projected onto a standard MRI template (*right*) (from [49])

There are mainly two kinds of ErRP, execution ErRP and observation ErRP [49]. When the subject is asked to respond as quickly as possible to a stimulus, execution ErRP arises if the subject makes an incorrect motor action. An example would be if the subject presses a key with the left hand when they should have responded with the right hand. The main components here are a negative potential appearing 80 ms after the incorrect response followed by a larger positive peak appearing 200–500 ms after the incorrect response. When the subject is asked to observe someone else performing a reaction task, an observation ErRP arises when the subject observes an error being made. Conveniently, these two types of ErRP can be distinguished in the EEG signals [49], as can be seen in Fig. 2.3. The main component of the observation ErRP is a negative potential 90 ms after the observed response, and peaking at 252 ms. The location in the brain of the observation ErRP is similar to the execution ErRP, as shown in Fig. 2.4.

In 2008, Pierre Ferrez and his colleagues tried to improve the control accuracy of a brain controlled mobile robot using ErRP [39] as shown in Fig. 2.5. After translating the subject's intention into a control command, the BCI displays the command, which will be executed only if there is no ErRP. Such a protocol depends on the ability to detect an ErRP quickly from a single trial, rather than by averaging a large number of trials [50]. To do this, they used a classifier trained on data recorded from the users up to three months earlier. They achieved an average recognition rate of 83.5% for single trials in cases where the BCI command was correct. For trials where the command was erroneous, and the ErRP appeared, the system detected it 79.2% of the time.

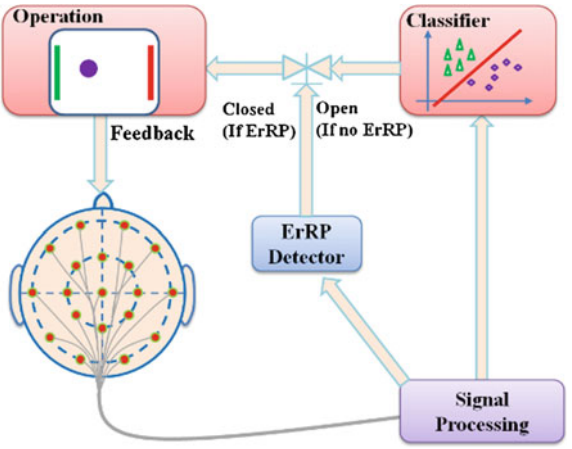

Fig. 2.5 A setup of a brain-controlled mobile robot using ErRP to improve accuracy. The subject receives visual feedback indicating the output of the classifier before the actual execution of the associated command (for example, "turn left"). If the feedback generates an ErRP, this command is simply ignored and the robot will continue executing the previous command. Otherwise, the command is sent to the robot

2.1.4 Current Limitations

In the past several decades, there have been many achievements in the area of EEG based BCI, such as control of a visual keyboard, cursor, wheelchair, smart home, and robotic arms. Nevertheless, few of them can be used in a practical environment outside the laboratory because of the following limitations.

Limited information transfer rate

The information transfer rate (ITR) from the user via a BCI to the outside world is not only limited by the immaturity of the technology, it can also be limited by the inherent characteristics of the EEG signal being observed. For example, the limited ITR of an SCP based BCI is inherent to the system (the SCP signal takes 1–2 s to change). Thus, unless a new signal source is used, the ITR and the response time of the BCI system are both limited.

On the other hand, the limited ITR of BCI based on SMR is likely due to the immaturity of the technology. The SMR signal is more complex, and contains higher frequency components. It is therefore likely that more information could be extracted with the right algorithm. However, current SMR-based BCIs can only detect slow changes in the SMR (similar to the slowly changing SCP signal).

Limited accuracy

The second obstacle for practical BCIs is their relatively low accuracy. This is not only due to the low identification rate of signal features. It is also because of fluctuations in the user's state of mind. Factors such as fatigue, illness, and change in attention can greatly affect the EEG signal. To improve overall accuracy, therefore, not only requires improvement of the classification accuracy in ideal circumstances, it must also be able to cope with changes in the user's state of mind. Designing a BCI system that relies on signals the user produces naturally will also mean less concentration is required, which may be less fatiguing to use and stabilise the user's state of mind.

Lack of user initiated switch

Present BCI systems primarily rely on protocols that begin at fixed times set by the system. However, in real life applications, BCIs in which the start and stop of operation is determined by the user are preferable. Without a mechanical safety cut-off switch, operation in daily life could be dangerous. Efforts to develop such a user-initiated switch, based on detection of certain features in the EEG have begun [51]. However, there are many unexplored options, and the mode of detection may be heavily influenced by the individual abilities of the user.

Different EEG patterns in different users

There are very significant differences in the EEG between different users—especially when neurological disorders, psychological issues, and damage to the brain are considered. To create a universal classification algorithm that suits every user may be impossible. Therefore, highly effective training methods that can match a new user after a short training session are important.

2.2 EMG and the Neuromuscular Interface

EMG signals are electrical activity generated when muscles are stimulated by the CNS. EMG information reflects the functional state of muscles, so it can be used for sensing the body's state of motion and predicting future actions. Cavanagh and Komi [52] studied human EMG signals. They experimentally showed that muscle contractions always occur 20–80 ms after their stimulating action potential appears, as measured by EMG. Therefore, EMG measures the electrical signals that excite muscles to generate force. EMG can be used to recognise human movement patterns, especially in the joint motion identification of the upper and lower limb. Meanwhile, as a nerve stimulation signal, it can also contribute to further applications in human rehabilitation therapy. Some examples of input interfaces, including EMG-based interfaces, are shown in Fig. 2.6.

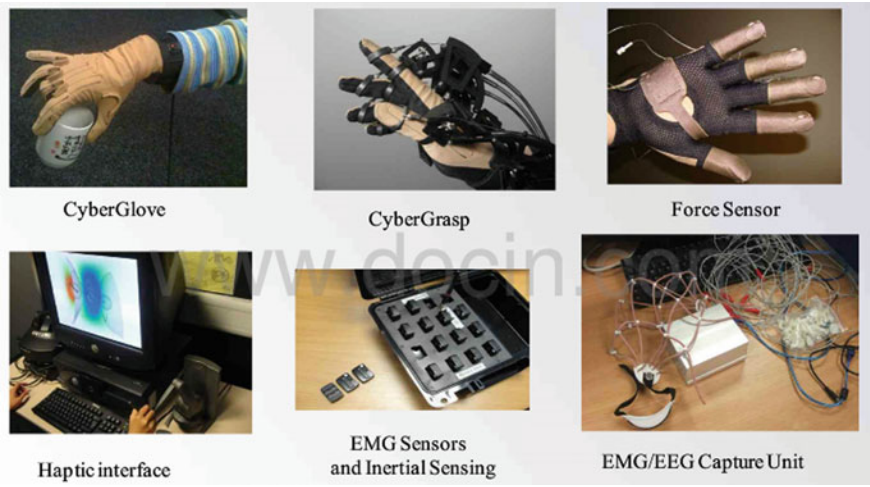

Fig. 2.6 Examples of input interface technologies

2.2.1 Applications of sEMG

Under controlled conditions, changes in sEMG signal can quantitatively reflect muscle activity. These changes are also indicators of important muscle activation features that describe muscle strength, muscle activation patterns, motor unit conduction velocity, muscle fatigue, and coordination between different muscles. Hence, EMG is closely associated with the functional state of muscles. Since it can reflect neuromuscular activity, sEMG has great theoretical significance and practical value in a number of areas.

Sport research

Sports research investigates human physical activity in sports and dance. Athletes' physical characteristics indicate their degree of physical exertion and their underlying muscle function. Monitoring these characteristics and referring to the results can be used to design proper training programs to improve athletes' performance. For example, sEMG can be used to determine the electro-mechanical delay in human activities, and the mechanisms behind muscles' biological recovery and changes in the brain's psychological state. Studying sEMG results also allows the sequence of muscle activation and muscle force to be assessed. Hence, analysis of these sEMG measurements can be used to improve human athletic performance.

Medical research

Based on the electrophysiological properties of nerves and muscles, and by using the electrical stimulation of nerves, researchers have used EMG to diagnose neuromuscular diseases. This method has been successful in treating chronic nonspecific back pain, scoliosis, stroke, and Parkinson's.

In 2004, Cheung et al. tested 30 adolescent idiopathic scoliosis patients and concluded that the ratio of the growth rate of the spine and sEMG signals can be used to assess the progression of adolescent idiopathic scoliosis [53]. Wu et al. tested 37 patients who were suffering from lumbar disc herniation. They compared the differences in sEMG signal from the vertical spine muscle and the multifidus before and after treatment [54]. The results showed that sEMG can be used as one of the objective indicators of clinical efficacy evaluation of lumbar disc herniation and has good clinical value. Neblett et al. [55] used sEMG and ROM (range of motion) to measure and evaluate the lumbar flexion relaxation effect. This effect means that the EMG signals of the extended muscles are similar to those in the rest state when the lumbar is in maximum flexion. They found that all normal subjects exhibited the flexion relaxation effect. In the 1980s, Kralj and Bajd put a hand control device into the paralysed patients' walking aids and fused the walking aids and an electrically stimulated neural prosthetic [56]. Later, the ParaCare team in Zurich University invented a hand function recovery system based on the EMG signal electrically stimulated neural prosthesis. It acquired EMG signals from the deltoid muscle in the shoulder [57]. Functional electrical stimulation (FES), as used in these devices, can help patients complete an explicit task, and is a promising technology in the recovery of limb function.

Rehabilitation research

In the design and control system of exoskeletons, prostheses, wheelchairs, and other assistive devices, sEMG signals are used as the control source by interpreting the movement intention of these devices' users. In exoskeleton technologies, Yoshiyuki Sankai, at the University of Tsukuba, developed the HAL (Hybrid Assistive Limb) system, which was designed to assist in walking and gait rehabilitation. It uses sEMG and ground reaction force measurements to predict its user's intention [58]. The University of Michigan built a rehabilitation device that used EMG signals from the calf soleus. They established a linear relationship between the EMG signals and muscle force that enabled them to control leg movement [59], as shown in Fig. 2.7. German company Ottobock developed an EMG controlled prosthetic hand (SUVA), which can easily and naturally open and close depending on the strength of the user's EMG signals [60, 61].

Gesture recognition and human-computer interaction

Gesture recognition uses sensors to detect a physical gesture and pattern recognition to determine the type of the gesture from those sensors' measurements. An EMG-based gesture control system collects sEMG signals and uses the data to identify different hand gestures and control devices. The data is passed through a pattern recogniser to return real-time high level gesture information as well as the joint's flexion angle and strength. The high level information includes the shape, position, and orientation of the gesture. Surface EMG has been used for a variety of computer interface gesture based control tasks, including assistive device control, automatic sign language translation, and interactive gaming.

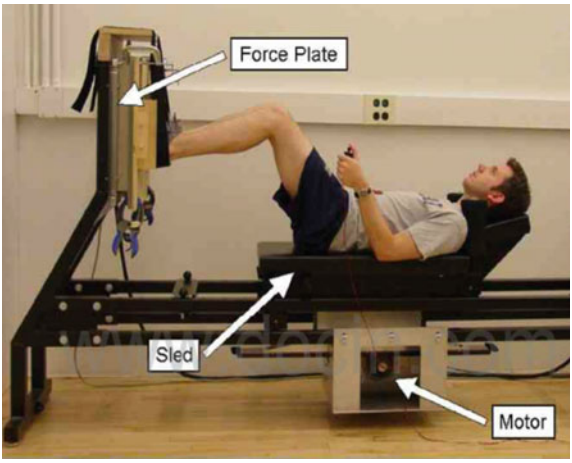

Fig. 2.7 The University of Michigan's rehabilitation robot

Surface EMG-based gesture recognition is not easily influenced by environmental factors, and it is lightweight, convenient, and inexpensive. These characteristics make it well suited for use in the home. For example, Jong-Sung et al. used six wrist gestures to achieve real-time control of a computer mouse with sEMG signals and gesture recognition [62]. Costanza et al. successfully controlled a phone by analysing different EMG signals [63]. Aso et al. used sEMG recognition results of hand and neck movements to control an electric car [64]. Wheeler developed a virtual joystick based on the sEMG gesture recognition, to control aircraft flight in a computer game [65, 66]. He also improved the number of classified gestures to nine kinds of wrist and finger movements, as shown in Fig. 2.8. Surface EMG can identify specific actions before they occur, improving the speed of the

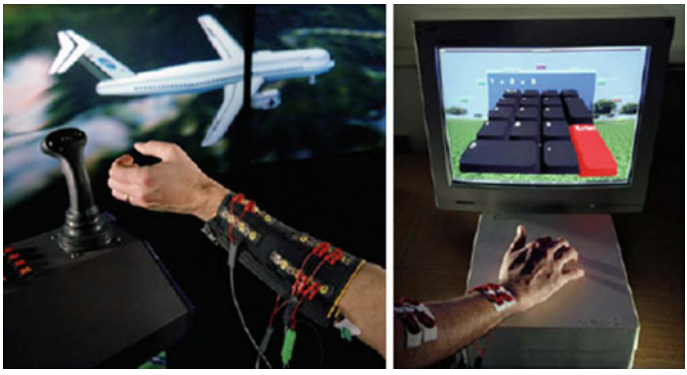

Fig. 2.8 Virtual joystick based on sEMG gesture recognition

human-computer interface. This is relevant to military and racing applications where short response times are required. In these applications the user who has the quicker interface gains an advantage.

2.2.2 sEMG-Based Neuromuscular Interface

EMG has been used as an input to a musculoskeletal model for isometric and dynamic tasks at different anatomical locations such as the elbow [67–69], shoulder [70], knee [71], ankle [72], jaw, lower back [73, 74], and wrist [75]. In these studies the aim was to estimate individual muscle forces by combining accurate EMG signal measurements and biomechanics models.

Buchanan et al. [76] used forward and inverse dynamics to cross-validate a forward model. From more than 200 knee flexion and extension torque tests, they found that the calibrated EMG-driven model made good predictions with an average R^2 of 0.91 ± 0.04. In addition, if the muscle-tendon parameters were kept constant, and only the EMG activation parameters adjusted, the model accurately predicted joint angle over an extended period. However, this model required offline tuning and was time-consuming to compute. This meant it could not be used for real-time operation.

Knaepen et al. [77] noted that before an EMG-driven model could be used as a reliable tool to estimate muscle force, it needed to be tested in a variety of situations. Koo and Mak first determined individual parameters for the musculotendon model. These were based on a set of nine elbow maximum isometric flexion locations in steps of 15° across the range of 0–120°. After calibration they used the same set of parameters and EMG signals as inputs to the model. By comparing the accuracy and consistency of the model, Koo and Mak predicted the effectiveness and versatility of the model during different dynamic sports activities.

Knaepen et al. [77] used univariate variance analysis to show the model accuracy was task-dependent. In a first task with voluntary loading during elbow flexion, they used the linear envelope method to get an RMSE of 13.71 ± 5.89°. In a second task with voluntary unloading during elbow extension the RMSE was 34.64 ± 7.79°. With voluntary unloading during elbow flexion the RMSE was 18.67 ± 8.49°.

Cavallaro [78] established an EMG driven interface to control a seven DOF upper limb exoskeleton. He used maximum error, RMSE, correlation coefficient, and the percentage of time of the absolute error below a specific threshold value to assess the model's predictive capabilities. He also established a functional relationship between the model task execution time (TET) and the number of modelling muscles.

Shao et al. [79] improved the model presented in [76]. He added viscous resistance to the muscle contraction kinetics ($F_{VE} = F_{Max} \times b_m \times v \times \cos \varphi$), and used the parallel SAA as its tuning method.

Sartori et al. [80] presented two methods to achieve real-time modelling. One was the high stiffness tendon treatment, which reduced computation time. The second was a new data processing method that reduced memory requirements. They achieved this by using a 2D cubic spline interpolation, instead of a four dimensional (4D) musculotendon estimated value interpolation method. They ran the model in real-time by placing all the EMG-driven models under the common SIMM framework.

Lloyd and Besier [71] found that their model could accurately predict a single cycle movement (average RMSE of 6.53°). However, when there was more than one cycle of movement, accuracy reduced to an average RMSE of 22°. This was because EMG signals have a low reproducibility and the same movement can be generated by a different pattern of EMG signals. This means the same tuning algorithm may not be suitable in different usage scenarios.

2.2.3 Current Challenges

Literature shows a great improvement in the interface development in recent years. However, there are still some gaps preventing the transfer of these EMG-based interfaces from an experimental environment to practical applications.

Quality of EMG

EMG is time and person dependent. An EMG-based human-robot interface needs to effectively process sEMG signals by extracting appropriate features and eliminating noise. Currently, filtering techniques are in the time-domain (such as mean value and RMSE), frequency domain (such as the median frequency, MF), and time-frequency domain (such as wavelet transform).

The advantage of the time-domain methods is their computational simplicity. The disadvantage is their poor identification reliability, because their character changes greatly when the muscle contraction changes. However, they have been widely used, because of their simplicity. Current prosthetic hands are controlled by time domain methods. Features in time domain methods include the integral of absolute value (IVA), zero crossing (ZC), variance (VAR), histogram of EMG (HEMG), integrated EMG value (iEMG), and RMSE.

The advantage of the frequency domain method is that the description of EMG in the frequency domain is relatively stable, which aids pattern recognition. The disadvantage is that the traditional FT can only characterise the overall frequency characteristics of the signal, and there are no time-resolved features. Thus, it can only be applied to the analysis of stationary signals. The commonly used frequency domain characteristics are the mean power frequency (MPF), MF, and power spectrum.

The time-frequency domain method incorporates time and frequency domain information. It has been received progressively more attention in the analysis of

non-stationary signals. Commonly used time-frequency methods include the short-time FT, wavelet transform, Wigner-Ville transform, and Choi-Williams transformation.

Channels of EMG

The contribution of each of the muscles to the overall torque of a joint is different. Hence, a significant challenge in designing the input of a human-robot interface is selecting a suitable number of muscle signals from each joint.

Knaepen et al. [77] tested the seven muscles that wrap around the elbow joint. The muscles are the biceps brachii long head, the biceps brachii short head, the brachioradialis, the triceps brachii longus, the triceps brachii lateralis, the triceps brachii medialis, and the anconeus. They found that for unloaded flexion, the activation of the biceps brachii and brachioradialis is quite small, and the brachialis contributes most to flexion. In loaded flexion, other elbow flexors start working alongside the brachialis. Koo and Mak also found that different flexor and extensor muscles contribute to smooth motion of the elbow joint. Their research did neither fully model the interaction between different muscles and their model was not accurate in real-time. This may be due to the unreliable nature of the brachialis EMG signal during elbow extension.

Choosing a suitable electrode is another challenge. The size of electrode should ideally be big enough to cover the whole muscle surface. However, an electrode of that size would pickup crosstalk from adjacent muscles. Meanwhile, some muscles (such as the brachialis) are covered by others, and the sEMG of these muscles cannot be measured directly. The standard of maximum endurance of musculoskeletal function has been used to predict brachialis' function [57]. This technique may allow for reduced numbers of required sEMG electrodes for satisfactory torque predictions.

Accuracy of model

At present, the predictive ability of the human-robot interface is limited. The RMSE of the model from Koo and Mak was 34.64 $\pm$ 7.79° in single cycle elbow flexion, and 18.67 $\pm$ 8.49° in single cycle extension [77]. Au and Kirsch tested the shoulder and elbow, but the movement RMSE was about 20° and the elbow RMSE was 19.6 $\pm$ 5.9° [81]. Artemiadis and Kyriakopoulos achieved a better result, an RMSE of 1.76–9.0° for arm movement limited to the horizontal plane [82]. The model from Pau et al. [83, 84] had an average RMSE of 4.18–10.1° in single cycle elbow motion. However, for multi-cycle, continuous, motion their model's accuracy reduced, as indicated by an RMSE of 15.98–36.06°. They also found significant variability between individuals. The problem of low accuracy of the interface is related to three aspects. First, the accuracy of the model's components, including signal processing, activation kinetics, muscle contraction dynamics, musculoskeletal geometry, and kinematics. Second, the human-robot interface feedback mechanism, and third, the online tuning algorithm.

2.3 Neuromusculoskeletal Models for Gait Rehabilitation

Gait rehabilitation robots interact with humans physically and cognitively. Thus, the design of human-robot control strategies can be improved by incorporating the human's intention, a patient-specific musculoskeletal system, and the biomechanical principles of human locomotion.

2.3.1 Musculoskeletal Model

The state-of-the-art musculoskeletal models are normally subject-specific interactive graphic-based geometrical models [85, 86]. They are used to obtain muscle-tendon properties, muscle-tendon kinematics, muscle-tendon dynamics, and the anatomical and anthropometric parameters of body segments. They are usually scaled from generic models by employing musculoskeletal modelling and simulation tools. The generic model defines the bone surfaces of the pelvis, femur, patella, tibia, fibula, and foot. The model also defines the joint kinematics of the lower limbs and the musculotendon paths of those muscles of lower limbs. The bone surfaces provided by SIMM, OpenSim [85], or Anybody [87] are usually obtained by digitisng a male skeleton with known anthropometric dimensions. The musculotendon paths of those selected muscles are modelled as a series of points connected by line segments. The musculotendon paths also include muscle origin and insertion points as well as additional intermediate points, which are defined when the muscle wraps over a joint surface. The patient-specific musculoskeletal model is scaled from the generic model based on the patient's anatomical parameters. The accurate anatomical information of each subject is usually obtained through a three dimensional (3D) motion capture system such as VICON (Oxford Metrics, UK).

Muscle force estimation

Understanding the forces applied to a joint and estimating how these forces are distributed among surrounding muscles, ligaments, and articular surfaces are fundamental to understand joint function, injury, and disease. Inverse dynamics can also be used to calculate the external load applied to a joint. However, given the indeterminate nature of a joint's external constraints, the contribution from muscles to support or move this load is far more difficult to determine.

Individual muscle forces during walking give in-depth information on neural control and tissue loading of gait. The individual muscle forces thus contribute to improve the diagnosis and management of neurological or orthopaedic conditions. Direct measurement of individual muscle forces is difficult. Minimal invasive measurements only estimate muscle forces in superficial tendons such as the Achilles [88, 89]. Direct measurements of muscle forces can also be achieved by placing force transducers on tendons during surgery [90]. In sum, non-invasive methods based on a musculoskeletal model are needed. However, estimation of

individual muscle forces in vivo is a challenging task because the human musculoskeletal system is a highly redundant system.

Static optimisation

There are many studies employing static optimisation algorithms to study individual muscle forces in the lower limbs during walking. Seireg and Arvikar [91] predicted muscle forces of 31 muscle groups and 7 segments from lower extremities, based on minimisation of the weighted sum of muscle forces and the moments at all joints. The resultant muscle forces were consistent with typical EMG patterns of level walking from the literature. Crowninshield and Brand [92], Crowninshield et al. [93] estimated muscle forces of 27 and 47 muscle groups around the hip, knee, and ankle joints by minimising the sum of different powers of muscle stresses. They also tested the sensitivity of the power of the objective function and found that a power of three was the most appropriate. They also found that muscle force patterns were not sensitive to small changes in objective function power.

Yamaguchi and Zajac [94] estimated muscle forces of 31 muscle groups of the lower limbs by minimising the sum of muscle forces and the mechanical-chemical power. They found that incomplete information on the physiological function and individual muscles caused large errors for accurate determination of muscle forces. Röhrle et al. [95] predicted individual muscle forces for 42 muscle groups and six DOFs by minimising the sum of muscle forces. The sensitivity of muscle origin and insertion points to muscle forces and joint forces was analysed. The results show that muscle origin and insertion points are more sensitive to joint forces.

Brand et al. [96] investigated the sensitivity of physiological cross-sectional area to muscle force by using a musculoskeletal model consisting of 47 muscle groups located around three joints. Other research groups also investigated the influence of different objective functions on muscle force prediction. Collins [97] calculated muscle forces from seven muscle groups around three joints by minimising sum of muscle forces (or the sum of muscle forces squared), muscle stresses, ligament forces, contact forces, and instantaneous muscle power. Results show that minimisation of total ligament force cannot successfully predict muscle activation when compared to EMG signals.

Some studies focus on muscle force prediction of knee joint flexion and extension using static optimisation. Dul et al. [98] compared the characteristics and performance of different objective functions for static-isometric knee flexion. The results show that linear objective functions predict discrete muscle activation, whereas nonlinear objective functions predict more realistic muscle activation. Li et al. [99] also tested the effectiveness of using different objective functions to predict muscle forces from ten muscle groups during isometric knee flexion and extension. The experiments show that linear, nonlinear, and physiological objective functions can all predict antagonistic muscle forces. The performance of muscle force prediction was more sensitive to kinematic information than to objective function. Forster et al. [100] studied and predicted co-contraction of antagonistic muscles in the knee joint.

Dynamic optimisation

Dynamic optimisation is not subject to the limitations of static optimisation and can ideally produce more realistic muscle forces. Delp et al. [85] solved muscle force sharing problems using dynamic optimisation by minimising tracking error and metabolic energy consumption. The method was validated using a typical static optimisation algorithm and EMG signal values taken from literature. Yamaguchi and Zajac [94] performed normal gait simulation by including ten muscle groups and eight DOFs of the lower limb. The objective function minimised tracking error and the sum of cubed muscle stress. Koo and Mak [86] examined individual muscle contributions of the ankle plantar flexors to actuate body segments during support, forward progression, and swing initiation.

Dynamic optimisation is not sensitive to kinematics data and can accurately represent the underlying physiological properties of the system. However, the multiple integrations make the algorithm computationally expensive. Therefore, it is not suitable for clinical or real-time applications. Previous studies show that static optimisation and dynamic optimisation can yield similar accuracy for muscle forces computed for human gait [93]. Applications that need to be computationally efficient can consider static optimisation, which estimates individual muscle forces in vivo and at the same time accounts for physiological properties.

2.3.2 EMG-Driven Models

Another approach to estimating muscle forces in vivo uses EMG in conjunction with appropriate musculoskeletal and muscle mechanics model to estimate forces. Since EMG-driven models rely on measured muscle activity to estimate muscle force, they implicitly account for a subject's individual activation patterns without the need to satisfy any constraints imposed by objective functions.

The EMG signals provide an indirect indicator of muscular function. The electric signals, which accompany the chemical stimulation of the muscle fibres, travel through the muscle and adjacent soft tissues. With appropriate instrumentation, these myoelectric signals can be recorded and analysed to determine timing and relative intensity of the muscular effort. In some circumstances, one can also estimate the resulting muscle forces. Also, EMG information is one of the best indicators of muscle activity for patients with neurological lesions that impair voluntary control. These include the spastic disabilities of cerebral palsy, stroke, brain injury, and spinal cord injury [101, 102].

Anatomical based EMG-driven models

Anatomically based EMG-driven models are based on Zajac's [103] musculotendon actuator model, the classical Hill-type model, and anatomical musculoskeletal models [103]. Previous EMG-driven models of varying complexity have been used to estimate kinetics (the individual muscle forces and joint moments [104]) and

joint kinematics (the joint angle, velocity, and acceleration [105, 106]). Such EMG-driven models include three main parts: the anatomical musculoskeletal model providing musculotendon length and muscle moment arms for selected muscles; the activation dynamics model converting raw EMG signals to muscle activations; and the muscle contraction dynamics converting the muscle activation to muscle forces [107].

Bogey et al. [107] developed an EMG-driven ankle model based on a generic musculoskeletal geometric model. Musculotendon parameters such as the maximum muscle isometric force, optimal muscle fibre length, muscle pennation angle, and muscle tendon length were adopted from anatomical studies [108]. Their model had good agreement with the ankle moment calculated by inverse dynamics. One reason could be that the participants were average size adult males who closely matched the generic anatomical musculoskeletal model. This model could not account for individual variations and is likely to be less accurate for other subjects. Gradually more models are employing the patient-specific musculoskeletal model to account for individual variability and a subject's own anatomical properties [104, 105]. These patient-specific musculoskeletal models are based on computer-interactive 3D musculoskeletal models and then scaled to the subjects using anatomical landmarks [109].

Most anatomical based EMG-driven models predict joint moments and individual muscle forces with an acceptable accuracy for a single DOF. For example, using one DOF EMG-driven models, Bogey et al. [107] and Shao et al. [110] modelled ankle dorsiflexion and plantar flexion, Lloyd and Besier [104] modelled knee flexion and extension, and Manual et al. [106] modelled elbow flexion and extension. Among these one-DOF EMG-driven models, some estimate the joint moment and muscle forces to be robust across a variety of tasks. Lloyd and Besier [104] performed maximum isometric contractions for flexors and extensors, eccentric hamstring and quadriceps contraction, low effort flexion and extension, combined flexion and extension with dynamometer tasks, and running trials (including a straight run, sidestep, and a crossover cut).

Multi-DOF EMG-driven models are developed to generate a more realistic representation of muscle activation patterns, muscle forces, or joint moments during a number of dynamics tasks. Sartori et al. [111, 112] developed a multi-DOF EMG-driven model using EMG signals recorded from 16 muscles driving 34 musculotendon actuators in nine dynamic tasks. These tasks were walking, running, sidestepping and crossover, hip adduction-abduction, hip flexion-extension, hip internal-external rotation, knee flexion-extension, ankle dorsi-plantar flexion, and ankle subtalar movement. The results show that the model generated muscle forces satisfying all DOF simultaneously. The model also has great potential to predict more physiologically accurate muscle forces than those predicted by previous single DOF EMG-driven models.

Some EMG-driven models can be modified for older patients [113] or patients with neurological disorders [110]. Thelen [113] used adjustable parameters (muscle deactivation time constant, isometric strength, maximum contraction velocity, maximum normalised force, and passive muscle strain due to maximum isometric

force) to account for changes in muscle properties with aging. Shao et al. [110] developed an EMG-driven model to estimate the muscle forces and joint moment of the ankle joint for stroke patients. Instead of adjusting the musculotendon mechanical parameters in the force-length-velocity (FLV) relationship and tendon strain-length relationship [110], they modified four muscle activation dynamics parameters and four parameters of muscle contraction dynamics. These parameters included the optimal muscle fibre length, tendon slack length, global percentage change in optimal muscle fibre length, and the maximum isometric force. Their modification accounts for the altered muscle activation and movement patterns of stroke patients.

Non-anatomical based EMG-driven models

Not all EMG-driven models are based on anatomical musculoskeletal models. Pau et al. [114, 115] developed a one DOF EMG-driven model for estimating elbow flexion and extension angle. This model was based on a simplified geometric model that treated the elbow joint as a single hinge with a fixed centre of rotation actuated by two main muscle groups. The muscle moment arms and musculotendon lengths were calculated using trigonometry. Pau et al.'s model also simplified the musculotendon model by including only muscle fibres. Although they predicted elbow joint angle with an acceptable performance, the simplifications on the musculoskeletal model and the musculotendon model make it difficult to adapt this model to the lower limb. Ding et al. [116] developed an EMG-driven state space model for the elbow joint with only one muscle actuator. This model did not include musculoskeletal, anatomical, or geometric details. The EMG-driven state space model combined the Hill-type model with joint forward dynamics, which mapped muscle activations to the joint motion. Two EMG features, the IVA and waveform length, were used to estimate elbow joint velocities and angle with an Extended Kalman Filter (EKF).

EMG-driven models designed for robotic applications

There is an increasing interest in employing EMG-driven models in gait rehabilitation robots. For instance, Song et al. [117] developed real-time EMG-driven arm wrestling robots to estimate individual muscle forces with EMG signals. They used wavelet packet transformation and an autoregressive model to extract EMG characteristics. An artificial NN was used to map the EMG signal to elbow joint force. Ryu et al. [118] developed an EMG-driven controller to replicate the wrist movement by estimating the wrist joint angle with EMG signals. The model obtained "quasi-tension" by performing signal processing. A supervised multi-layer neural network trained by a back-propagation algorithm was used to estimate wrist angle. They claimed that their model improved the effectiveness of a teleoperated robotic manipulator.

In some cases, modifications were made to existing anatomical based EMG-driven models for real-time robotic applications. Sartori et al. [119] made a set of enhancements to reduce their model's computation time and memory

requirements, allowing for real-time control of a lower limb powered orthosis. They designed a more efficient algorithm, which allowed the integration of all sub-models into a single framework and reduced the demand for memory to achieve real-time calculation. First, they replaced the elastic tendon of the Hill-type muscle model with a stiff tendon. Second, they created three different 2D tables per muscle to store subject-specific musculotendon length values calculated with SIMM. At each run the tables were indexed based on the current joint positions.

Some EMG-driven models are integrated with virtual reality technology to give bio-feedback for those who are limbless, have congenital defects, or require rehabilitation. Patients are familiarised with their new limb and movement ability in a virtual training environment. AI-Jumaily and Olivares [120] developed an EMG-driven below-shoulder 3D human arm integrated with virtual reality. Their model was based on signal classification and anatomical structure with virtual reality modelling. Sartori et al. [121] developed a 3D virtual model of the lower limb for potential use with a real-time EMG-driven gait rehabilitation exoskeleton. They developed a graphical interface, which allowed the user to visualise the skeletal geometry and the movement driving it.

2.4 Discussion

Over the past 25 years, many productive BCI research programmes have been developed. As EEG systems are portable and almost all other brain activity recording technologies are not, the former have great potential to underpin the implementation of BCIs in daily life. In addition, EEG-based BCIs are probably the best choice for a practical BCI because of their relatively low cost, high temporal resolution, and low clinical risk.

As the previous sections have shown, BCI research so far consists primarily of demonstrations and limited studies. These show that a specific brain signal, processed in a specific way, can create a simple output. BCI development, however, is still in the earliest stages, and it is difficult to tell how far away a BCI for the masses or the disabled is. According to Wolpaw [122] and other researchers [123], there are several issues that significantly affect the development of BCIs: (a), interpreting the internal aspects of normal brain function; (b), new signal acquisition, processing, and classification techniques; (c), exploring the largely unknown potential and limitations of non-muscular communication; (d), psychological and behavioural factors that affect user motivation and success; (e), adoption of standard research techniques and evaluation criteria; (f), appropriate choice of applications and user groups; (g), development of user training strategies; (h), initial switches controlled by users; (i), the convenience, safety, and stability of the complete system; and (j), cost, appearance, marketing, and regulatory concerns.

So far, many EEG-based prototypes have been demonstrated in laboratories for applications such as cursor control, visual keyboards, and mind controlled

wheelchairs and prosthetics. As the first generation of EEG-based BCIs, their limitations are obvious. First, almost all of the prototypes have only been demonstrated in laboratories, not the real world. Second, their operation speed and accuracy are too low for them to be useful in most cases. Finally, all current systems can only operate with the supervision of researchers. Without the introduction of intelligent limitations and safety systems, current BCIs could be unpredictable or even dangerous to use independently.

Neuromusculoskeletal models have the potential to improve the effectiveness of gait rehabilitation robots by modelling patient's dynamics more accurately and detecting the patient's intention. The review shows that the subject-specific musculoskeletal models [85] provide accurate anatomical or anthropometric parameters of segments. The models can also provide patient-specific muscle parameters or musculotendon kinematics. These parameters could be used to model a patient's dynamics accurately. Individual muscle forces, regarded as a patient's intention or active muscle effort, can be estimated in vivo by optimisation algorithms [91, 92] or EMG-driven models [104–107].

Practice has shown that EMG signals are significantly affected by fatigue. The amplitude and spectral energy of sEMG signals are closely related to muscle fatigue. Petrofsky and Phillips [124] studied the relationship between sEMG and muscle temperature, muscle fatigue, and muscle blood flow under conditions of muscle isovolumetric contraction. The results showed that blood flow has little effect on the sEMG amplitude and frequency, and that temperature and muscle fatigue reduce the frequency and increase the amplitude of sEMG signals.

The main methods to assess fatigue are the root mean square value (RMS), MF, and MPF. Moritani et al. [125] found that, under normal circumstances, the Fourier spectrum curve of sEMG may be shifted to the left by muscle fatigue. This caused the MPF and MF to decrease. Park and Meek tried to consider the issue of fatigue [126]. Their work focused on the tuning of particular interface parameters but requires feedback.

2.5 Summary

This chapter presented a review of existing works relevant to BCIs and neuromuscular interfaces. Numerous issues in the development of biomechatronics for rehabilitation have been identified and there is much room for improvement. Of particular concern is the inability of the BCIs, neural interfaces, and musculoskeletal models to achieve their advanced applications for medical rehabilitation devices. The different types of bio-signals driven models and interfaces developed in the literature were considered. Subsequently, studies relating to human kinematics and computational modelling were also examined. The state of the art of biomechanical interfaces for rehabilitation robots was reviewed.

References

1. Kübler, A., et al., Brain-computer communication: Unlocking the locked in. Psychological Bulletin, 2001. 127(3): p. 358–375.
2. Birbaumer, N., et al., A spelling device for the paralysed. Nature, 1999. 398(6725): p. 297–298.
3. Farwell, L.A. and E. Donchin, Talking off the top of your head - Toward a mental prosthesis utilizing event-related brain potentials. Electroencephalography and Clinical Neurophysiology, 1988. 70(6): p. 510–523.
4. Donchin, E., K.M. Spencer, and R. Wijesinghe, The mental prosthesis: assessing the speed of a P300-based brain-computer interface. IEEE Transactions on Rehabilitation Engineering, 2000. 8(2): p. 174–179.
5. Wolpaw, J.R. and D.J. McFarland, Control of a two-dimensional movement signal by a noninvasive brain-computer interface in humans. Proceedings of the National Academy of Sciences of the United States of America, 2004. 101(51): p. 17849–54.
6. McFarland, D.J., et al., Mu and beta rhythm topographies during motor imagery and actual movements. Brain Topography, 2000. 12(3): p. 177–186.
7. Kostov, A. and M. Polak, Parallel man-machine training in development of EEG-based cursor control. IEEE Transactions in Rehabilitation Engineering, 2000. 8(2): p. 203–205.
8. Wolpaw, J.R. and D.J. Mcfarland, Multichannel EEG-Based brain-computer communication. Electroencephalography and Clinical Neurophysiology, 1994. 90(6): p. 444–449.
9. Wolpaw, J.R., et al., The Wadsworth Center brain-computer interface (BCI) research and development program. IEEE Transactions on Neural Systems and Rehabilitation Engineering, 2003. 11(2): p. 204–207.
10. Niedermeyer, E. and F.L.d. Silva, Electroencephalography Basic Principles, Clinical Applications, and Related Fields. 5th ed. 2004: Lippincott Williams & Wilkins. 1256 pages.
11. Wolpaw, J. and E.W. Wolpaw, Brain-Computer Interfaces: Principles and Practice. 1 ed. 2012: Oxford University Press.
12. Guangyu, B., et al., VEP-based brain-computer interfaces: Time, frequency, and code modulations. IEEE Computational Intelligence Magazine, 2009. 4(4): p. 22–26.
13. Sutter, E.E., The brain response interface: Communication through visually-induced electrical brain responses. Journal of Microcomputer Applications, 1992. 15(1): p. 31–45.
14. Trejo, L.J., R. Rosipal, and B. Matthews, Brain-computer interfaces for 1-D and 2-D cursor control: Designs using volitional control of the EEG spectrum or steady-state visual evoked potentials. IEEE Transactions on Neural Systems and Rehabilitation Engineering, 2006. 14 (2): p. 225–229.
15. Martinez, P., H. Bakardjian, and A. Cichocki, Fully online multicommand brain-computer interface with visual neurofeedback using SSVEP paradigm. Computational Intelligence and Neuroscience & Biobehavioral Reviews, 2007. 2007: p. 9.
16. Faller, J., et al., Avatar navigation in virtual and augmented reality environments using an SSVEP BCI. in International Conference on Applied Bionics and Biomechanics 2010: Venice, Italy. p. 1–4.
17. McDaid, A.J., S. Xing, and S.Q. Xie. Brain controlled robotic exoskeleton for neurorehabilitation. in 2013 IEEE/ASME International Conference on Advanced Intelligent Mechatronics, 2013. Wollongong, Australia.
18. Song, X., S.Q. Xie, and K.C. Aw, EEG-based brain computer interface for game control, in International Conference on Affective Computing and Intelligent Interaction. 2012: Taipei, Taiwan. p. 47–54.
19. Kelly, S.P., et al., Visual spatial attention tracking using high-density SSVEP data for independent brain-computer communication. IEEE Transactions on Neural Systems and Rehabilitation Engineering, 2005. 13(2): p. 172–178.
20. Allison, B.Z., et al., Towards an independent brain-computer interface using steady state visual evoked potentials. Clinical Neurophysiology, 2008. 119(2): p. 399–408.

21. Goncharova, I.I., et al., EMG contamination of EEG: Spectral and topographical characteristics. Clinical Neurophysiology, 2003. 114(9): p. 1580–1593.
22. Fatourechi, M., et al., EMG and EOG artifacts in brain computer interface systems: A survey. Clinical Neurophysiology, 2007. 118(3): p. 480–494.
23. Anderer, P., et al., Artifact processing in computerized analysis of sleep EEG – A review. Neuropsychobiology, 1999. 40(3): p. 150–157.
24. Jung, T.-P., et al., Removal of eye activity artifacts from visual event-related potentials in normal and clinical subjects. Clinical Neurophysiology, 2000. 111(10): p. 1745–1758.
25. McFarland, D.J., et al., Spatial filter selection for EEG-based communication. Electroencephalography and Clinical Neurophysiology, 1997. 103(3): p. 386–394.
26. Gupta, S. and H. Singh. Preprocessing EEG signals for direct human-system interface. in IEEE International Joint Symposia on Intelligence and Systems, 1996.
27. Bostanov, V., BCI competition 2003-Data sets Ib and IIb: Feature extraction from event-related brain potentials with the continuous wavelet transform and the t-value scalogram. IEEE Transactions on Biomedical Engineering, 2004. 51(6): p. 1057–1061.
28. Lei, Q. and H. Bin, A wavelet-based time–frequency analysis approach for classification of motor imagery for brain–computer interface applications. Journal of Neural Engineering, 2005. 2(4): p. 65.
29. Garcia, G.N., T. Ebrahimi, and J.M. Vesin. Correlative exploration of EEG signals for direct brain-computer communication. in IEEE International Conference on Acoustics, Speech, and Signal, 2003.
30. Flotzinger, D., M. Pregenzer, and G. Pfurtscheller. Feature selection with distinction sensitive learning vector quantisation and genetic algorithms. in IEEE World Congress on Computational Intelligence, 1994.
31. Pregenzer, M. and G. Pfurtscheller, Frequency component selection for an EEG-based brain to computer interface. IEEE Transactions on Rehabilitation Engineering, 1999. 7(4): p. 413–419.
32. Chaiyaratana, N. and A.M.S. Zalzala. Recent developments in evolutionary and genetic algorithms: Theory and applications. in Genetic Algorithms in Engineering Systems: Innovations and Applications, 1997.
33. Müller, K.R., C.W. Anderson, and G.E. Birch, Linear and nonlinear methods for brain-computer interfaces. IEEE Transactions on Neural Systems and Rehabilitation Engineering, 2003. 11(2): p. 165–169.
34. Bayliss, J.D., S.A. Inverso, and A. Tentler, Changing the P300 brain computer interface. Cyberpsychology & Behavior, 2004. 7(6): p. 694–704.
35. Anderson, C.W., E.A. Stolz, and S. Shamsunder, Multivariate autoregressive models for classification of spontaneous electroencephalographic signals during mental tasks. IEEE Transactions on Biomedical Engineering, 1998. 45(3): p. 277–286.
36. Palaniappan, R. Brain computer interface design using band powers extracted during mental tasks. in IEEE EMBS Conference on Neural Engineering, 2005.
37. Peterson, D.A., et al., Feature selection and blind source separation in an EEG-based brain-computer interface. Journal on Applied Signal Processing, 2005. 2005(19): p. 3128–3140.
38. Haselsteiner, E. and G. Pfurtscheller, Using time-dependent neural networks for EEG classification. IEEE Transactions on Rehabilitation Engineering, 2000. 8(4): p. 457–63.
39. Ferrez, P.W. and J. del R. Millan, Error-related EEG potentials generated during simulated brain-computer interaction. IEEE Transactions on Biomedical Engineering, 2008. 55(3): p. 923–929.
40. Wolpaw, J.R., et al., EEG-based communication: Improved accuracy by response verification. IEEE Transactions on Rehabilitation Engineering, 1998. 6(3): p. 326–333.
41. Millan, J.d., et al. Neural networks for robust classification of mental tasks. in Proceedings of the 22nd Annual International Conference of the IEEE Engineering in Medicine and Biology Society, 2000.

42. Millan, J.R., et al., A local neural classifier for the recognition of EEG patterns associated to mental tasks. IEEE Transactions on Neural Networks, 2002. 13(3): p. 678–686.
43. Peters, B.O., G. Pfurtscheller, and H. Flyvbjerg, Automatic differentiation of multichannel EEG signals. IEEE Transactions on Biomedical Engineering, 2001. 48(1): p. 111–116.
44. McFarland, D.J., L.M. McCane, and J.R. Wolpaw, EEG-based communication and control: Short-term role of feedback. IEEE Transactions on Rehabilitation Engineering, 1998. 6(1): p. 7–11.
45. Siniatchkin, M., P. Kropp, and W.-D. Gerber, Neurofeedback—The significance of reinforcement and the search for an appropriate strategy for the success of self-regulation. Applied Psychophysiology and Biofeedback, 2000. 25(3): p. 167–175.
46. Carter, C.S., et al., The role of the anterior cingulate cortex in error detection and the on-line monitoring of performance: An event related fMRI study. Biological Psychiatry, 1998. 43: p. 13s.
47. Carter, C.S., et al., Anterior cingulate cortex, error detection, and the online monitoring of performance. Science, 1998. 280(5364): p. 747–749.
48. Holroyd, C.B. and M.G.H. Coles, The neural basis of human error processing: Reinforcement learning, dopamine and the error-related negativity. Psychological Review, 2002. 109(4): p. 679–709.
49. van Schie, H.T., et al., Modulation of activity in medial frontal and motor cortices during error observation. Nature Neuroscience, 2004. 7(5): p. 549–554.
50. Schalk, G., et al., EEG-based communication: Presence of an error potential. Clinical Neurophysiology, 2000. 111(12): p. 2138–2144.
51. Mason, S.G. and G.E. Birch, A general framework for brain-computer interface design. IEEE Transactions on Neural Systems and Rehabilitation Engineering, 2003. 11(1): p. 70–85.
52. Cavanagh P.R., and P.V. Komi, Electromechanical delay in human skeletal muscle under concentric and eccentric contractions. European Journal of Applied Physiology and Occupational Physiology, 1979. 42(3): p. 159–163.
53. Cheung K.M., et al., Recent advances in the aetiology of adolescent idiopathic scoliosis. International Orthopaedics, 2008. 32(6): p. 729–734.
54. Wu W., et al., Application of surface EMG in evaluation of effectiveness of clinical interventions for lumbar intervertebral disc prolapse. Chinese Journal of Physical Medicine and Rehabilitation, 2002. 9.
55. Neblett R., et al., A clinical guide to surface-EMG-assisted stretching as an adjunct to chronic musculoskeletal pain rehabilitation. Applied Psychophysiology and Biofeedback, 2003. 28(2): p. 147–160.
56. Kralj A.R., and T. Bajd, Functional electrical stimulation: Standing and walking after spinal cord injury: CRC press, 1989.
57. Jezernik S., et al., Robotic orthosis lokomat: A rehabilitation and research tool. Neuromodulation, 2003. 6(2): p. 108–115.
58. Sankai Y., HAL: Hybrid assistive limb based on cybernics. Robotics Research, 2010. p. 25–34.
59. Huston L.J., and E.M. Wojtys, Neuromuscular performance characteristics in elite female athletes. The American Journal of Sports Medicine, 1996. 24(4): p. 427–436, 1996.
60. Lovely R.C.-D., Commercial Hardware for the Implementation of Myoelectric Control. Powered Upper Limb Prostheses: Control, Implementation and Clinical Application, 2004.
61. Huang Z.-X., X.-D. Zhang, and Y.-N. Li, Design of a grasp force adaptive control system with tactile and slip perception. in IEEE International Conference on Automation Science and Engineering, August 20–24, 2012. p. 1101–1105.
62. Jong-Sung K., Huyk J., and Wookho S., A new means of HCI: EMG-MOUSE. in IEEE International Conference on Systems, Man and Cybernetics, October 10–13, 2004. p. 100–104.

63. Costanza E., S.A. Inverso, and R. Allen, Toward subtle intimate interfaces for mobile devices using an EMG controller. in Proceedings of the SIGCHI Conference on Human Factors in Computing Systems, 2005. p. 481–489.
64. Aso S., et al., Driving electric car by using EMG interface. IEEE Conference on Cybernetics and Intelligent Systems, June 7–9, 2006. p. 1–5.
65. Wheeler K.R., and C.C. Jorgensen, Gestures as input: Neuroelectric joysticks and keyboards. IEEE Pervasive Computing, 2003. 2(2): p. 56–61.
66. Wheeler K.R., Device control using gestures sensed from EMG. in IEEE International Workshop on Soft Computing in Industrial Applications, June 22–25, 2003. p. 21–26.
67. Feng C.J., A.F. Mak, and T.K. Koo, A surface EMG driven musculoskeletal model of the elbow flexion-extension movement in normal subjects and in subjects with spasticity. Journal of Musculoskeletal Research, 1999. 3(2): p. 109–123.
68. Buchanan T., S. Delp, and J. Solbeck, Muscular resistance to varus and valgus loads at the elbow. Journal of Biomechanical Engineering, 1998. 120(5): p. 634.
69. Soechting J., and M. Flanders, Evaluating an integrated musculoskeletal model of the human arm. Journal of Biomechanical Engineering, 1997. 119(1): p. 93.
70. Laursen B., B.R. Jensen, G. Németh, and G. Sjøgaard, A model predicting individual shoulder muscle forces based on relationship between electromyographic and 3D external forces in static position. Journal of Biomechanics, 1998. 31(8): p. 731.
71. Lloyd D.G., and T.F. Besier, An EMG-driven musculoskeletal model to estimate muscle forces and knee joint moments in vivo. Journal of Biomechanics, 2003. 36(6): p. 765–776.
72. Ferris D.P., et al., An improved powered ankle–foot orthosis using proportional myoelectric control. Gait & Posture, 2006. 23(4): p. 425–428.
73. Granata K.P., and W. Marras, An EMG-assisted model of trunk loading during free-dynamic lifting. Journal of Biomechanics, 1995. 28(11): p. 1309–1317.
74. Nussbaum M.A., and D.B. Chaffin, Lumbar muscle force estimation using a subject-invariant 5-parameter EMG-based model. Journal of Biomechanics, 1998. 31(7): p. 667–672.
75. Buchanan T.S., et al., Estimation of muscle forces about the wrist joint during isometric tasks using an EMG coefficient method. Journal of Biomechanics, 1993. 26(4–5): p. 547–560.
76. Buchanan T.S., et al., Neuromusculoskeletal modeling: Estimation of muscle forces and joint moments and movements from measurements of neural command. Journal of Applied Biomechanics, 2004. 20(4): p. 367–395.
77. Knaepen, K., et al., Human-robot interaction: Kinematics and muscle activity inside a powered compliant knee exoskeleton. IEEE Transactions on Neural Systems and Rehabilitation Engineering, 2014.
78. Cavallaro F., Fuzzy TOPSIS approach for assessing thermal-energy storage in concentrated solar power (CSP) systems, Applied Energy, vol. 87, no. 2, p. 496–503, 2010.
79. Shao Q., et al., An EMG-driven model to estimate muscle forces and joint moments in stroke patients. Computers in Biology and Medicine, 2009. 39(12): p. 1083–1088.
80. Sartori M., et al., Fast operation of anatomical and stiff tendon neuromuscular models in EMG-driven modeling. in IEEE International Conference on Robotics and Automation, 2010. p. 2228–2234.
81. Au A.T., and R.F. Kirsch, EMG-based prediction of shoulder and elbow kinematics in able-bodied and spinal cord injured individuals. IEEE Transactions on Rehabilitation Engineering, 2000. 8(4): p. 471–480, 2000.
82. Artemiadis P.K., and K.J. Kyriakopoulos, EMG-based control of a robot arm using low-dimensional embeddings. IEEE Transactions on Robotics, 2010. 26(2): p. 393–398.
83. Pau J.W., S.Q. Xie, and A.J. Pullan, Neuromuscular interfacing: Establishing an EMG-driven model for the human elbow joint. IEEE Transactions on Biomedical Engineering, 2012. 59(9): p. 2586–2593.

84. Pau J.W.L., et al., An EMG-driven neuromuscular interface for human elbow joint. 3rd IEEE RAS and EMBS International Conference on Biomedical Robotics and Biomechatronics, September 26–29, 2010. p. 156-161.
85. Delp, S.L., et al., An interactive graphics-based model of the lower extremity to study orthopaedic surgical procedures. IEEE Transactions on Biomedical Engineering, 1990. 37(8): p. 757–767.
86. Koo, T.K.K. and A.F.T. Mak, Feasibility of using EMG driven neuromusculoskeletal model for prediction of dynamic movement of the elbow. Journal of Electromyography and Kinesiology, 2005. 15(1): p. 12–26.
87. Damsgaard, M., et al., Analysis of musculoskeletal systems in the AnyBody Modeling System. Simulation Modelling Practice and Theory, 2006. 14(8): p. 1100–1111.
88. Finni, T., P.V. Komi, and J. Lukkariniemi, Achilles tendon loading during walking: Application of a novel optic fiber technique. European Journal of Applied Physiology and Occupational Physiology, 1998. 77(3): p. 289–291.
89. Komi, P.V., S. Fukashiro, and M. Järvinen, Biomechanical loading of Achilles tendon during normal locomotion. Clinics in Sports Medicine, 1992. 11(3): p. 521–531.
90. Dennerlein, J.T., et al., Tensions of the flexor digitorum superficialis are higher than a current model predicts. Journal of biomechanics, 1998. 31(4): p. 295–301.
91. Seireg, A. and R.J. Arvikar, The prediction of muscular load sharing and joint forces in the lower extremities during walking. Journal of Biomechanics, 1975. 8(2): p. 89–102.
92. Crowninshield, R.D. and R.A. Brand, A physiologically based criterion of muscle force prediction in locomotion. Journal of Biomechanics, 1981. 14(11): p. 793–801.
93. Crowninshield, R.D., et al., A biomechanical investigation of the human hip. Journal of Biomechanics, 1978. 11(1–2): p. 75–85.
94. Yamaguchi, G.T. and F.E. Zajac, Restoring unassisted natural gait to paraplegics via functional neuromuscular stimulation: A computer simulation study. IEEE Transactions on Biomedical Engineering, 1990. 37(9): p. 886–902.
95. Röhrle, H., et al., Joint forces in the human pelvis-leg skeleton during walking. Journal of Biomechanics, 1984. 17(6): p. 409–424.
96. Brand, R.A., D.R. Pedersen, and J.A. Friederich, The sensitivity of muscle force predictions to changes in physiologic cross-sectional area. Journal of Biomechanics, 1986. 19(8): p. 589–596.
97. Collins, J.J., The redundant nature of locomotor optimization laws. Journal of Biomechanics, 1995. 28(3): p. 251–267.
98. Dul, J., et al., Muscular synergism—I. On criteria for load sharing between synergistic muscles. Journal of Biomechanics, 1984. 17(9): p. 663–673.
99. Li, G., et al., Prediction of antagonistic muscle forces using inverse dynamic optimization during flexion/extension of the knee. Journal of Biomechanical Engineering, 1999. 121(3): p. 316–322.
100. Forster, E., et al., Extension of a state-of-the-art optimization criterion to predict co-contraction. Journal of Biomechanics, 2004. 37(4): p. 577–581.
101. Knutsson, E. and C. Richards, Different types of disturbed motor control in gait of hemiparetic patients. Brain, 1979. 102(2): p. 405–430.
102. Perry J., et al., Gait analysis of the triceps surae in cerebral palsy: A preoperative and postoperative clinical and electromyographic study. Journal of Bone & Joint Surgery, 1974. 56(3): p. 511–520.
103. Zajac, F.E., Muscle and tendon: Properties, models, scaling, and application to biomechanics and motor control. Critical Reviews in Biomedical Engineering, 1989. 17(4): p. 359–411.
104. Carozza, M. C., et al. “On the development of a novel adaptive prosthetic hand with compliant joints: experimental platform and EMG control.” 2005 IEEE/RSJ International Conference on Intelligent Robots and Systems. IEEE, 2005.
105. Yang, Da-peng, et al. “An anthropomorphic robot hand developed based on underactuated mechanism and controlled by EMG signals.” Journal of Bionic Engineering, 2009, 6(3): p. 255–263.

106. Manal, K., et al., A real-time EMG-driven virtual arm. Computers in Biology and Medicine, 2002. 32(1): p. 25–36.
107. Bogey, R.A., J. Perry, and A.J. Gitter, An EMG-to-force processing approach for determining ankle muscle forces during normal human gait. IEEE Transactions on Neural Systems and Rehabilitation Engineering, 2005. 13(3): p. 302–310.
108. Gordon, A., A.F. Huxley, and F. Julian, The variation in isometric tension with sarcomere length in vertebrate muscle fibres. The Journal of physiology, 1966. 184(1): p. 170–192.
109. Buchanan, T.S., et al., Estimation of muscle forces and joint moments using a forward-inverse dynamics model. Medicine and Science in Sports and exercise, 2005. 37(11): p. 1911.
110. Tong, R. Biomechatronics in medicine and healthcare. Pan Stanford Publishing, 2011.
111. Sartori, M., et al. An EMG-driven musculoskeletal model of the human lower limb for the estimation of muscle forces and moments at the hip, knee and ankle joints in vivo. in Proceedings of International Conference on Simulation, Modeling and Programming for Autonomous Robots, 2010.
112. Sartori, M., et al., EMG-driven forward-dynamic estimation of muscle force and joint moment about multiple degrees of freedom in the human lower extremity. PloS one, 2012. 7(12): p. e52618.
113. Thelen, D.G., Adjustment of muscle mechanics model parameters to simulate dynamic contractions in older adults. Journal of Biomechanical Engineering, 2003. 125(1): p. 70–77.
114. Pau, J.W.L., et al., An EMG-driven neuromuscular interface for human elbow joint. in IEEE RAS and EMBS International Conference on Biomedical Robotics and Biomechatronics, 2010.
115. Carrozza MC, A wearable biomechatronic interface for controlling robots with voluntary foot movements. IEEE/ASME Transactions on Mechatronics. 2007, 12(1): p. 1–1.
116. Ding, Q.C., et al., A novel EMG-driven state space model for the estimation of continuous joint movements. in IEEE International Conference on Systems, Man, and Cybernetics, 2011.
117. Song, Q., et al., A real-time EMG-driven arm wrestling robot considering motion characteristics of human upper limbs. International Journal of Humanoid Robotics, 2007. 4(4): p. 645–670.
118. Ryu, W., B. Han, and J. Kim. Continuous position control of 1 DOF manipulator using EMG signals. in Third International Conference on Convergence and Hybrid Information Technology, 2008.
119. Jain R.K., Design and control of an IPMC artificial muscle finger for micro gripper using EMG signal. Mechatronics, 2013, 23(3): p. 381–94.
120. Al-Jumaily, A. and R.A. Olivares, Bio-driven system-based virtual reality for prosthetic and rehabilitation systems. Signal, Image and Video Processing, 2012. 6(1): p. 71–84.
121. Sartori, M., G. Chemello, and E. Pagello, A 3D virtual model of the knee driven by EMG signals. in Artificial Intelligence and Human-Oriented Computing, 2007. p. 591–601.
122. Wolpaw, J.R., et al., Brain-computer interfaces for communication and control. Clinical Neurophysiology, 2002. 113(6): p. 767–791.
123. Allison, B. and J. Jacko, The I of BCIs: Next Generation Interfaces for Brain–Computer Interface Systems That Adapt to Individual Users, in Human-Computer Interaction. Novel Interaction Methods and Techniques. 2009, Springer Berlin/ Heidelberg. p. 558–568.
124. Petrofsky J.S., and C.A. Phillips, Interactions between fatigue, muscle temperature, blood flow and the surface EMG. NAECON, 1980. p. 520–527.
125. Moritani T., M. Muro, and A. Nagata, Intramuscular and surface electromyogram changes during muscle fatigue. Journal of Applied Physiology, 1986. 60(4): p. 1179–1185.
126. Park E., and S.G. Meek, Fatigue compensation of the electromyographic signal for prosthetic control and force estimation. IEEE Transactions on Biomedical Engineering, 1993. 40(10): p. 1019–1023.

http://www.springer.com/978-3-319-52883-0

Biomechatronics in Medical Rehabilitation
Biomodelling, Interface, and Control
Xie, S.; Meng, W. (Eds.)
2017, XVIII, 203 p. 107 illus., 93 illus. in color.,
Hardcover
ISBN: 978-3-319-52883-0